INTERFACE

royalsocietypublishing.org/journal/rsif

Research

Cite this article: Narvaez JP, Yanoviak SP, Bitzer PM, Burchfield JC, Gora EM. 2024 Effects of urbanization on cloud-to-ground lightning strike frequency: a global perspective. *J. R. Soc. Interface* **21**: 20240257.
https://doi.org/10.1098/rsif.2024.0257

Received: 18 April 2024
Accepted: 12 August 2024

Subject Category:
Life Sciences–Earth Science interface

Subject Areas:
biophysics, environmental science, biogeography

Keywords:
lightning enhancement, urban systems, remote sensing, urban heat island, model averaging

Author for correspondence:
J. Pablo Narvaez
e-mail: pablo.narvaez@marquette.edu

Electronic supplementary material is available online at https://doi.org/10.6084/m9.figshare.c.7422806.

THE ROYAL SOCIETY PUBLISHING

Effects of urbanization on cloud-to-ground lightning strike frequency: a global perspective

J. Pablo Narvaez[1,2], Stephen P. Yanoviak[1,3], Phillip M. Bitzer[4], Jeffrey C. Burchfield[5] and Evan M. Gora[1,6]

[1]Smithsonian Tropical Research Institute, Apartado 0843-03092, Balboa, Panama
[2]Department of Biological Sciences, Marquette University, Milwaukee, WI 53201, USA
[3]Department of Biology, University of Louisville, 139 Life Sciences Building, Louisville, KY 40292, USA
[4]Department of Atmospheric and Earth Science, and [5]Earth System Science Center, The University of Alabama in Huntsville, Huntsville, AL 35899, USA
[6]Cary Institute of Ecosystem Studies, Millbrook, New York, NY 12545, USA

JPN, 0009-0004-3094-4309; SPY, 0000-0001-6425-1413; EMG, 0000-0002-0537-5835

Urbanization tends to increase local lightning frequency (i.e. the 'lightning enhancement' effect). Despite many urban areas showing lightning enhancement, the prevalence of these effects is unknown and the drivers underlying these patterns are poorly quantified. We conducted a global assessment of cloud-to-ground lightning flashes (lightning strikes) across 349 cities to evaluate how the likelihood and magnitude of lightning enhancement vary with geography, climate, air pollution, topography and urban development. The likelihood of exhibiting lightning enhancement increased with higher temperature and precipitation in urban areas relative to their natural surroundings (i.e. urban heat islands and elevated urban precipitation), higher regional lightning strike frequency, greater distance to water bodies and lower elevations. Lightning enhancement was stronger in cities with conspicuous heat islands and elevated urban precipitation effects, higher lightning strike frequency, larger urban areas and lower latitudes. The particularly strong effects of elevated urban temperature and precipitation indicate that these are dominant mechanisms by which cities cause local lightning enhancement.

1. Introduction

Lightning, particularly discharges that strike the ground (i.e. cloud-to-ground lightning), is an agent of death and destruction in natural and anthropogenic systems. Local lightning frequency increases with higher temperatures, greater fine aerosol concentrations, proximity to water bodies and the presence of tall, isolated objects ([1–3]; table 1). Many cities provide this exact combination of ingredients, and local lightning frequency tends to be higher in urban areas—a phenomenon referred to as the lightning enhancement effect ([3,16,17]; table 1). However, evidence for lightning enhancement is limited to a relatively small number of cities, and the mechanisms are either unclear or unknown in most cases. Fundamentally, because these studies compare one or a few cities with nearby landscapes that differ in a multitude of ways, the resulting patterns are confounded by multiple variables, including both measured and unmeasured factors. Thus, this study aimed to overcome these limitations by exploring global variation in lightning enhancement to determine (i) how widespread is the positive effect of urbanization on regional lightning strike frequency, and (ii) what characteristics of cities are most strongly associated with variation in the lightning enhancement effect.

Table 1. Review of studies investigating the urban lightning enhancement effect. 'Response' is the response variable used to measure lightning enhancement reported as lightning strike frequency (km^{-2}), total lightning (in-cloud lightning and lightning strikes, km^{-2}), Z-ratio (lightning strikes/total lightning), or lightning potential index (LPI, J kg^{-1}). 'Predictor(s)' refers to the variables that significantly predicted variation in the response reported as PM10 and PM2.5, particulate matter less than 10 and 2.5 µm in diameter, respectively); AOD, aerosol optical depth; CAPE, convective available potential energy; SO_2, sulfur dioxide concentration; SRH, surface relative humidity; UHI, urban heat island effect. 'Significant enhancement' is the fraction of cities that exhibited significant enhancement within each study.

city or region	response	significant predictor(s)	significant enhancement	reference
São Paulo and nearby cities (Brazil)	lightning strike frequency	PM10, UHI	3/3	[3]
Manaus (Brazil)	lightning strike frequency	UHI	1/1	[4]
Pearl River Delta megacity (China)	LPI, lightning strike frequency	AOD	1/1	[5]
Beijing (China)	lightning strike frequency	air temperature, SO_2, NO_2, PM2.5 and PM10	1/1	[6]
Chengdu, Wuhan and Jinan (China)	lightning strike frequency, Z-ratio	CAPE, SRH and AOD	3/3	[7]
Delhi, Mumbai, Bengaluru and Kolkata (India)	total lightning	AOD, UHI	1/4	[8]
Tel Aviv (Israel)	total lightning	aerosol concentration, AOD, PM25, PM10	1/1	[9]
Seoul (South Korea)	lightning strike frequency	PM10 and SO_2	1/1	[10]
Busan, Incheon, Daegu, Taejon and Gwangju (South Korea)	lightning strike frequency	PM10 and SO_2	5/5	[11]
Taipei (Taiwan)	lightning strike frequency	PM10 and SO_2	1/1	[12]
Central Spain	lightning strike ratio (upwind/downwind)	population, urban size, PM10 and SO_2	7/9	[13]
Midwestern (USA)	lightning strike frequency	pollution, topography	12/16	[1]
Houston, Texas (USA)	lightning strike frequency	PM10 and UHI	1/1	[2]
Northern Georgia (USA)	lightning strike frequency	distances from the nearest coal power plant and highways	1/1	[14]
Charlotte-Atlanta megaregion (USA)	total lightning	urban area, density and orientation.	2/3	[15]

Lightning enhancement is linked to air pollution and elevated temperatures associated with urban areas (table 1). Anthropogenic and naturally derived aerosols (e.g. sulfate and nitrate aerosol products from the combustion of fossil fuels and sea spray aerosols or volcanic ash, respectively) can alter within-cloud processes to increase lightning frequency [18–21]. Similarly, the urban heat island effect (i.e. the tendency for cities to be hotter than nearby natural environments [22]; can increase convection, thereby increasing lightning activity [23]. Although lightning enhancement is often statistically linked to aerosol concentrations or urban heat islands (9 of 12 studies for aerosols and three of four studies for urban heat islands; table 1 [10,11,13]), these factors are inherently confounded with other aspects of urbanization. Associations with these factors are unknown for most cities lacking lightning enhancement, perhaps due to the limited number of cities studied and potential biases in city selection (e.g. 100% of single-city studies reported enhancement, whereas 76.7% of cities exhibited enhancement in multi-city studies; table 1). This study addresses this problem by examining a large number of cities spanning wide variations in pollution, heat island effects and lightning enhancement.

Lightning enhancement is also influenced by geography, topography and associated climatic patterns. On a global scale, lightning frequency is highest near the equator, where temperatures and rainfall rates also tend to be high [24]. At more local geographic scales, lightning frequency tends to be high near water bodies [25–27], presumably due to abundant moisture and higher concentrations of fine particulate aerosols. Similarly, lightning frequency is particularly high in the foothills of some mountainous regions [28], indicating that topography influences lightning activity. These factors potentially interact with temperature and air pollution near urban centres to modulate the likelihood and magnitude of the lightning enhancement effect. However, the contribution of some of these factors (e.g. urban topography and population) is typically overlooked in urban lightning research [15].

Apart from these mechanistic drivers, the best predictors of urban lightning enhancement effects may be metrics of urbanization. Ultimately, the lightning enhancement effect is linked to urban development and its impact on the local climate. Thus, critical metrics of urban development, such as urban area, population size or the density of urbanization (i.e. the extent of natural cover within the urban areas), probably predict variation in the lightning enhancement effect (e.g. [13,29]). However, these relationships are untested.

Here, we quantify the distribution of urban lightning enhancement among 349 cities worldwide and explore the factors influencing the magnitude of enhancement. Specifically, we evaluate how urbanization influences lightning frequency within the boundaries of each city. Based on existing data and hypotheses described above, we predicted that urban lightning enhancement is more common and stronger where (i) urban heat islands are hotter, (ii) air has higher aerosols and particulate concentrations associated with pollution, (iii) urban areas are closer to water bodies, and (iv) cities cover more area or have greater populations. This study is unique in scope and scale because it captures global variation in urbanization and its effects on lightning enhancement. This approach does not measure physical processes within individual cities. However, it is unprecedented in its scale and, thus, its statistical power to separate the contributions of potentially confounding effects on lightning enhancement.

2. Methods

2.1. Lightning strike data

We quantified the urban lightning enhancement effect using Earth Networks Total Lightning Network (ENTLN) data. ENTLN continuously detects and locates lightning using each discharge's time and signal amplitude [30]; here, we focus on the ENTLN-classified cloud-to-ground flashes (or a group of strokes), which we call lightning strikes. We omitted lightning strikes less than 10 kA in magnitude to avoid misclassification with in-cloud lightning [31]. We calculated monthly mean lightning strike frequency (lightning strikes km^{-2} yr^{-1}) on a 0.05° × 0.05° grid (approximately 5 × 5 km) extending from 60° N to 60° S latitude for 2013–2020.

2.2. Urban and natural areas

We used the 2018 Moderate Resolution Imaging Spectroradiometer (MODIS) land cover data (MCD12C1 Version 6 [32]; on a 0.05° grid to identify urbanized land and its surrounding natural areas. The operational definition of a city used in this study was more than 300 000 inhabitants, based on the definition of a city in the UN World Urbanization Prospects [33]. We did not differentiate among various definitions of urban areas (e.g. city proper, urban agglomeration and metropolitan area), which probably introduces additional variation. Regardless, these were the best data available and suitable for capturing broad trends in population size. We omitted only five cities by limiting the data to within 60° N and 60° S latitude. Additionally, we did not evaluate the increase or decrease in the urban area during the 2013–2020 period. We assumed that the changes in area in most cities in the last decade are not significant enough to influence the lightning enhancement effect. Spatially, we defined cities as clusters of 0.05° × 0.05° cells with more than 50% urbanization overlapping the city centre, defined by the United Nations World's Cities in 2018–Data Booklet [33], or contiguous with other urban cells. Because the urbanization footprint of a city is often a mosaic of developed and undeveloped space (e.g. water bodies), we also included any cell with greater than 50% urban area that was within two cells of the city centre or contiguous city area (no cells of less than 50% urban area were included in a city). These adjacent and nearby urban cells collectively represented the urban area for each city (electronic supplementary material, figure S1a–c). This process collapsed 22 pairs of cities into single urban centres (e.g. Dallas/Ft. Worth, Philadelphia/Trenton). We identified 884 cities with more than 300 000 inhabitants and at least one cell comprising greater than 50% urban area.

We used MODIS to identify natural areas surrounding each city. Specifically, we defined natural areas as any combination of non-modified MODIS terrestrial layers: mixed forest, evergreen needleleaf forest, evergreen broadleaf forest, deciduous needleleaf forest, deciduous broadleaf forest, woody savannahs, savannahs, grasslands, closed shrublands, open shrublands, permanent wetlands, permanent snow and barren land (excluding water bodies, urban area and croplands) within 150 km of the boundaries of a city. We chose a 150 km radius because it is approximately 1/10 of the detection distance of this sensor system and therefore, should experience limited bias in detection efficiency across its area. Additionally, a buffer of 150 km captures sufficient area to estimate non-urban lightning frequency, and this radius was previously used to assess climatic differences between urban and non-urban pairs (e.g. urban island effect and pollution [34,35]). When a cell was within 150 km of multiple cities, we associated that natural area cell with the closest city. To limit edge effects, we removed all natural areas within two cells (approximately 10 km) of any cell with greater than 50% urban area (electronic supplementary material, figure S1d). We only retained cities in our dataset if they had at least 100 km^2 of associated natural area (691 cities qualified; electronic supplementary material, figure S2c). The natural areas capture the typical lightning frequency of each region with limited direct influence of urbanization, functioning as a reference point for evaluating the effect of each urban area.

2.3. Calculating lightning frequency

We calculated each pixel's average (i.e. the mean) annual lightning frequency using only months with meaningful lightning activity. We removed all cities with less than 1 lightning strike km^{-2} yr^{-1} in their associated natural areas. We also removed months from individual cities if their natural areas exhibited less than 1 lightning strike km^{-2} yr^{-1} in those months (328 cities removed). This approach was necessary for two reasons. First, we lacked the statistical power to test for urban enhancement when the lightning frequency is low, because the lightning frequency is strongly overdispersed and within-city sample sizes

Table 2. Predictor variables explain the variation of lighting enhancement along with their measurement method, units and source. All variables were upscaled or downscaled to the spatial grain of the lightning frequency data.

group	variable	units	temporal resolution (years covered)	spatial scale	data type	source
climate	regional lightning frequency	strikes km^{-2} yr^{-1}	monthly total (2013–2020)	0.05 × 0.05	electrical ground sensor network	[30]
	average air temperature	K (at 2 m above the surface from ERA5 data)	monthly averages of daily data (2013–2019)	0.05 × 0.05	reanalysis of weather station data	[37]
	maximum air temperature					
	minimum air temperature					
	local precipitation	kg m^{-2} $month^{-1}$	monthly total (2013–2018)	0.05 × 0.05		[37]
pollution	total aerosols	µm of particulates scaled from 0 to 1	monthly averages (2013–2020)	0.1 × 0.1	satellite sensors	[38]
	NO_2	billion molecules mm^{-2}		0.1 × 0.1		[39]
	SO_2	µg m^{-3}		0.625 × 0.5	reanalysis of satellite data	[40]
topography and geography	elevation	m	single measurement (2018)	3 arcsec (approximately 90 m)	satellite sensors	[41]
	distance to water bodies	km	single measurement (2021)	0.1 × 0.1	satellite sensors	[42]
urban characteristics	urban area	km^2	single measurement (2021)	0.05 × 0.05	satellite sensors	[32]
	population	1000s of inhabitants	single measurement (2018)	—	population census	[33]
	greenspace	percentage of natural area	single measurement (2021)	0.05 × 0.05	satellite sensors	[32]

were small. Second, removing low-frequency months avoided spurious effects resulting from uneven seasonality patterns (e.g. including all months would produce a latitudinal effect relating to season rather than the strength of urban enhancement). Additionally, we removed months and cities (eight cities in total) lacking data for their covariates (e.g. precipitation data was not available for 2019 and 2020, and the aerosol optical depth sensor could not make its measurement in certain areas during the study). Following these criteria, we ultimately included 349 cities in the analyses.

We used Glass's delta effect size and a simulation approach to evaluate whether each city exhibited unambiguous lightning enhancement. Glass's delta effect size is a statistical method for quantifying the magnitude of the difference between a treatment group (here, an urban area) and a control (nearby natural areas). To calculate Glass's delta, we divided the mean difference in lightning strike frequency (lightning strikes km^{-2} yr^{-1}) between urban and natural areas by the standard deviation of lightning strike frequency of the associated natural area. Glass's delta was preferable to other effect size metrics because the much larger sample size of the natural areas, relative to the cities, results in a more precise estimate of standard deviation (electronic supplementary material, figure S2a–c). Effect sizes greater than or equal to 0.5 were considered significant [36]. We confirmed that 218 of the 228 cities with effect sizes greater than 0.5 were also identified as significant using a simulation test based on random pulls from the natural area associated with each city. Specifically, we calculated the mean lightning strike frequency for random pulls of natural area cells (10 000 repetitions with the number of resampled natural cells equal to the number of urban cells). We confirmed that less than 5% of repetitions had an average lightning frequency equal to or greater than the observed lightning frequency in the urban area. We considered the 218 cities identified with both approaches as those exhibiting unambiguous lightning enhancement. This conservative approach probably eliminated false positives while potentially producing some false negatives.

The detection efficiency of ENTLN probably exhibits unquantifiable spatial biases. However, the spatial grain of these biases is much larger than that of our city and natural area measurements (150 km radius) because individual ENTLN sensors detect lightning over distances greater than 1000 km. Moreover, changes in network sensitivity over time will be experienced similarly by all city-specific pixels because of their proximity. We measured the strength of urban enhancement by dividing a city's average lightning strike frequency by the average lightning strike frequency in its associated natural area (hereafter, *urban–natural strike ratio*). Accordingly, this approach is insensitive to possible differences in detection efficiency among cities or over time.

2.4. Climatological, topographical and geographic covariates

We used spatially explicit, gridded data products to aggregate climatological, topographical and geographic covariates for each 0.05° × 0.05° cell (table 2). We assigned each 0.05° × 0.05° cell the proportional average of overlapping sulfur dioxide (SO_2) values because of the mismatch in resolution. All other data were downscaled or upscaled to the same spatial grain as the lightning data (table 2). Climate and pollution data were aggregated monthly. The temperature metrics captured monthly averages of daily trends and were advantageous because of their broad spatial coverage and fine resolution, but they did not capture detailed within-day variation, which could influence both rainfall and lightning activity [43]. All other variables had a single value because they did not change during the study period (e.g. topography) or data were limited (e.g. population).

We used these spatially explicit datasets to calculate potential predictors of variation in the lightning enhancement effect. For each variable described in table 2, we extracted its average value for each urban area during the months retained in the dataset (i.e. months with more than 1 lightning strike km^{-2} yr^{-1}). We calculated annual and cumulative averages of those values from 2013 to 2020. The only exception was regional lightning frequency, which equalled the mean lightning strike frequency across all natural and urban cells (i.e. the region). To assess the density of urbanization within each city, we calculated the percentage of land covered by natural areas within the urban cells of each city (hereafter greenspace). We also calculated the local effect of urbanization on temperature, precipitation and all aerosol variables. Specifically, we divided the average values of these predictors in the urban areas by their average across all cells in the associated natural areas, and we referred to these variables as the 'variable' ratio (e.g. temperature ratio or precipitation ratio). This allowed us to determine if lightning enhancement was directly associated with the effect of urbanization on local climate and pollution, such as the urban heat island effect (i.e. urban temperature divided by natural area temperature). We log-transformed overdispersed variables before analysis (12 of the 17 fixed-effect predictors were transformed; average temperature, local precipitation, total elevation, absolute latitude and greenspace were not transformed). Because the annual data for aerosol depth and urban–natural strike ratio included three and four zero values, respectively, we added half the smallest positive value (0.0020 for aerosol optical depth and 0.0446 for urban–natural strike ratio) to each variable before transformation.

2.5. Model averaging

We used Akaike information criterion (AIC) model averaging to explore spatio-temporal variation in the likelihood and magnitude of the lightning enhancement effect. This statistical method fits all possible models from the set of predictors and then blends predictions from the best-performing candidate models based on their goodness-of-fit (i.e. AIC scores), ultimately identifying fixed effects that consistently explain variation in the response variable. To evaluate the probability of enhancement, we constructed a generalized linear model with a binary response variable indicating whether there was lightning enhancement (determined by a threshold of Glass's delta greater than or equal to 0.5). This model included a single value for each city with 17 predictors averaged across all years (349 observations; table 2). To explore spatio-temporal variation in enhancement strength, we assessed how the urban–natural strike ratio varied among cities with unambiguous enhancement using annual data from 2013 to 2018 (218 cities with 1217 city-year observations). Specifically, we constructed a mixed-effect linear model (fitted with the lmer function of the lme4 package [44]; with an urban–natural strike ratio as the response variable, a random effect for the city (accounting for the annual lightning variation of each city), and the same collection of 17 fixed-effect predictors (table 2; representing the linear relationships between these predictors and the response variable). We used unique annual values for all variables with yearly data (i.e. all lightning, climate and pollution variables). We note that some variables were omitted from this final set of predictors (i.e. mean maximum temperature, mean minimum temperature, the ratios between urban and natural areas for these two variables and the total concentration of NO_2) because of collinearity, as determined by Pearson correlations ($R > 0.7$) and variance inflation factors (VIF > 5).

We fitted models for every possible combination of these terms (function dredge). Then, we averaged all models with AICc values within four of the lowest AICc values (function model.avg in package MuMIn [45]). We scaled all variables (Z-transformation) to allow direct comparison of coefficients, and we identified significant predictors as model-averaged coefficients with 95% confidence intervals (CI) that did not overlap with zero. Additionally, we performed forward model selection and assessed whether including pairwise interaction terms between the significant predictors decreased model AIC. We verified the appropriate model fit and the need for all transformations by evaluating model residuals (e.g. Q–Q plots). All analyses were conducted in the R statistical environment [46].

3. Results

Among the 349 cities with at least 1 lightning strike km^{-2} yr^{-1}, 218 exhibited unambiguous lightning enhancement based on the criteria used in this study (figure 1*a*,*b*). The likelihood of exhibiting unambiguous lightning enhancement increased with increasing regional lightning strike frequency, stronger urban heat island effects, higher precipitation ratios (i.e. local precipitation divided by natural area precipitation), larger distance to water bodies and lower elevation (figures 2 and 3*a*–*e*; electronic supplementary material, tables S1 and S3). However, the likelihood of enhancement was not associated with average temperature, local precipitation, pollution, other topographic and geographic variables or any metrics of urbanization. There were no interactions among the significant predictors identified with model averaging.

The effects of lightning enhancement were particularly strong in some cities. Urban lightning strike frequency was more than double nearby natural areas in 46.8% of cities with enhancement (102 of 218), with a maximum of 10 times more lightning

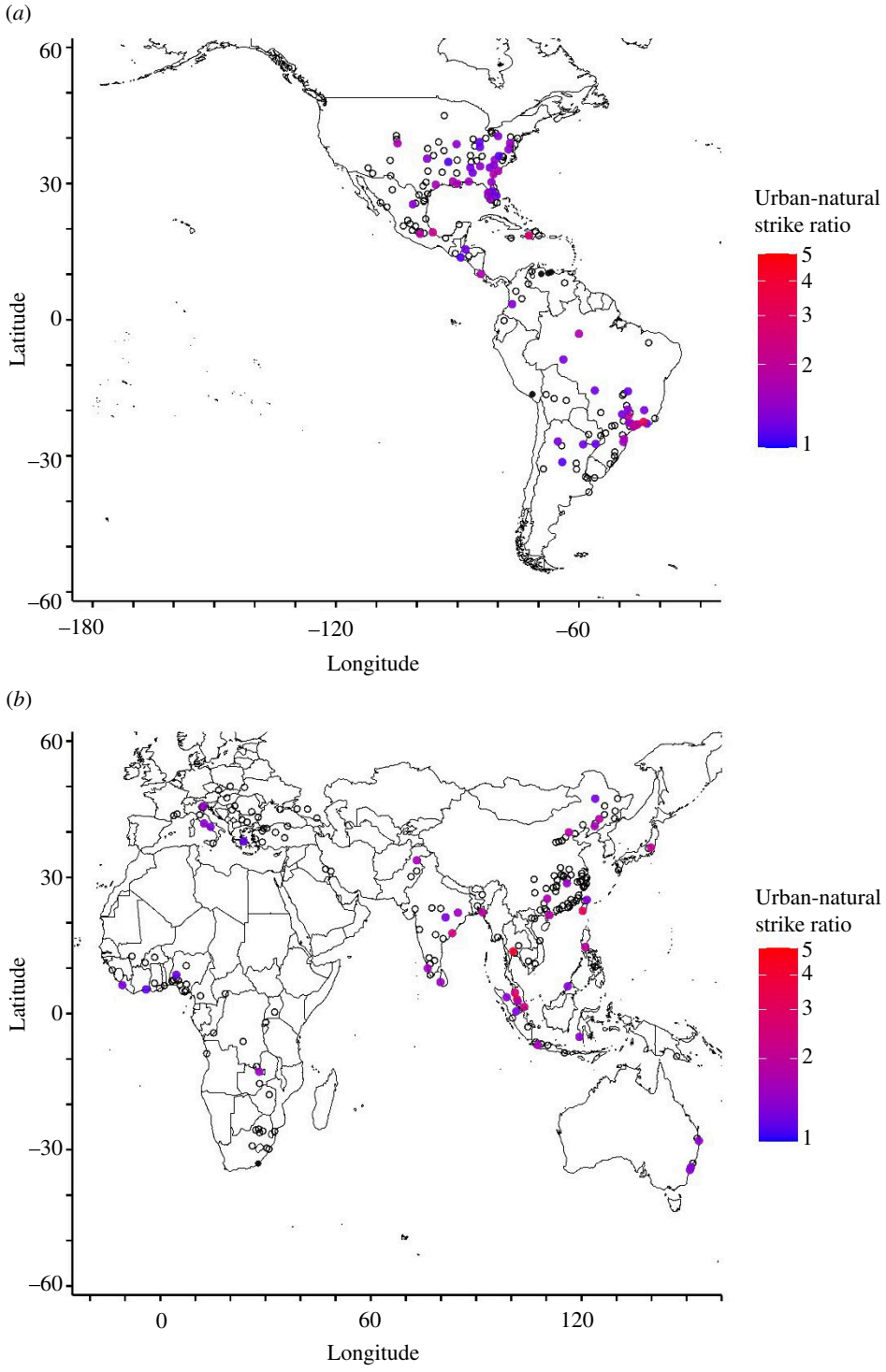

Figure 1. The global distribution of cities (more than 300 000 inhabitants) and variation in the strength of urban lightning enhancement are split approximately between the Western Hemisphere (*a*) and the Eastern Hemisphere (*b*). Black points represent cities with low regional lightning strike frequencies (less than 1 strike km^{-2} yr^{-1}), and empty circles represent cities without urban lightning enhancement (less than 0.5 Glass's delta). Coloured points represent cities with significant lightning enhancement (greater than or equal to 0.5 Glass's delta) shaded by the strength of enhancement (i.e. urban–natural strike ratio).

strikes in the urban area of Baoding, China, compared with its natural surroundings in 2020 (16.2 versus 1.6 lightning strikes km^{-2} yr^{-1} in its urban and natural area, respectively; figure 2*f*). Among cities with significant lightning enhancement, the urban–natural strike ratio (i.e. the magnitude of enhancement) increased with higher regional lightning strike frequency, strong urban heat island effects, higher precipitation ratios, larger urban areas and at lower latitudes. However, the strength of urban lightning enhancement did not change with pollution, other climate and topographic variables or other urban characteristics (figure 2; electronic supplementary material, figure S3a–d, tables S1 and S3).

The effects of higher precipitation ratios (i.e. urban precipitation relative to their natural areas) and urban area were modified by interactions with other variables (electronic supplementary material, figure S4a–c, tables S1 and S3). The impact of increased precipitation ratios on the strength of lightning enhancement was greater in regions with higher overall lightning strike frequency and among cities located in higher latitudes. By contrast, the effect of urban area on the strength of lightning

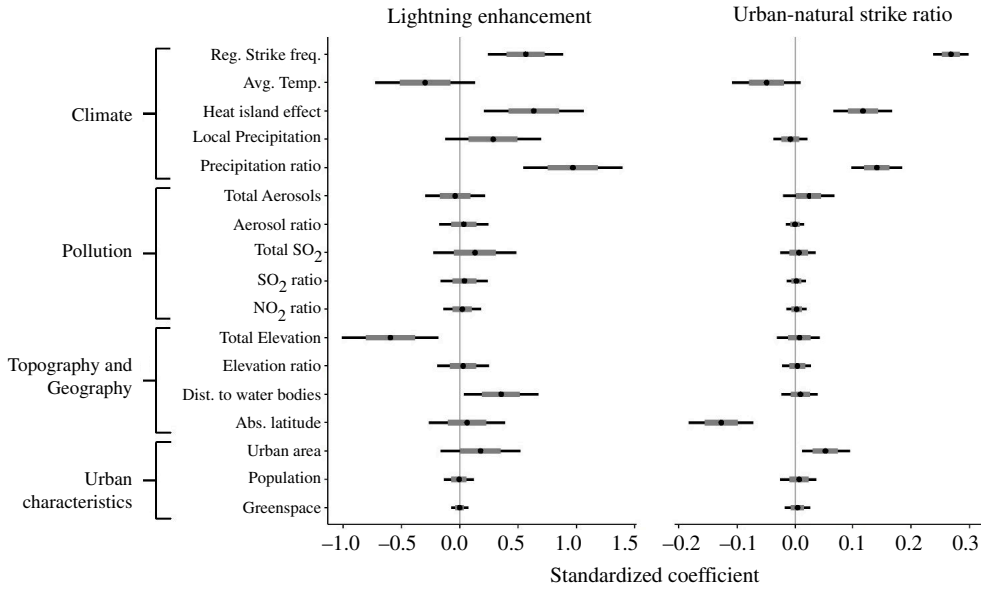

Figure 2. Model-averaged relationships between the likelihood and magnitude of lightning enhancement (i.e. the urban–natural strike ratio) with the different explanatory variables. The black dots are the estimated value of the predictors, the grey bars are their standard error and the black lines depict their 95% CI. If the 95% CI for a given term overlaps with the zero line, then that indicates that the modelled effect was not significantly different from zero.

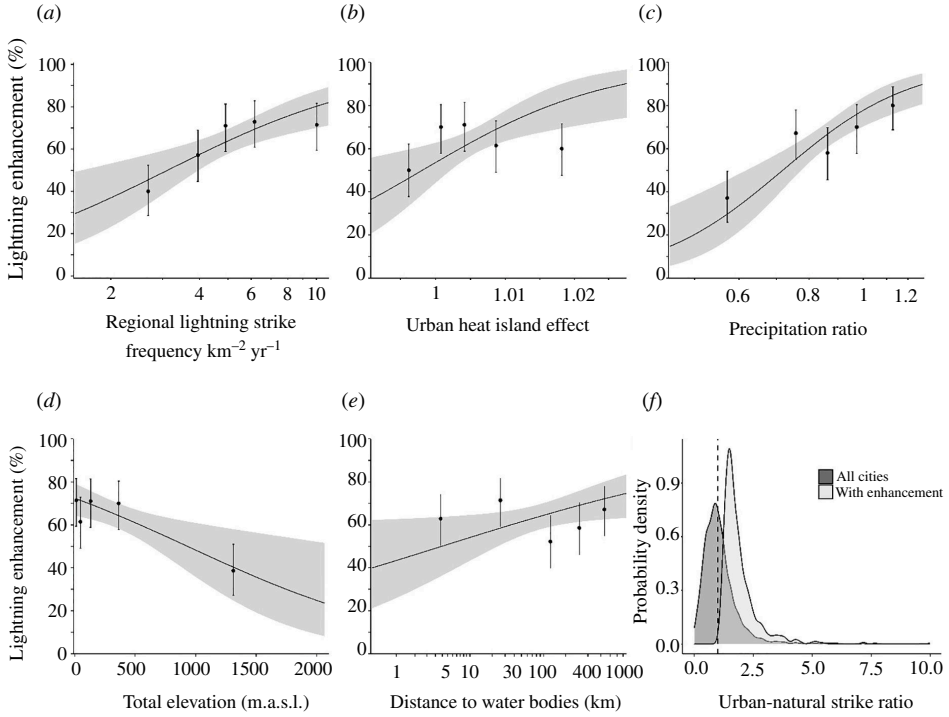

Figure 3. Variation in lightning enhancement with significant predictors from the AIC model averaging analysis (*a*) regional lightning strike frequency (km^{-2} yr^{-1}); (*b*) urban heat island effect; (*c*) precipitation ratio; (*d*) total elevation (m.a.s.l.); (*e*) distance to water bodies). The regression lines represent the model averaging slopes for each predictor and lightning enhancement. The shaded portions represent the 95% CI of each regression line. Lightning enhancement was binned into quantiles to allow visualization of model fit to the binary response variable. (*f*) Shows a density plot representing the probability density of the urban–natural strike ratio for all cities and cities with unambiguous lightning enhancement. The dashed line represents the value at which urban and natural lightning strike frequency equals.

enhancement was lessened in regions with high lightning strike frequency. There were no significant interactions among other predictors.

4. Discussion

Here, we provide the first global assessment of urban lightning enhancement and its drivers. Increased local lightning strike frequency occurred in at least 218 major cities worldwide, with extremely strong effects in a subset of those cities. However, we also show that not all urban areas had detectable lightning enhancement effects. The results indicate that urban heat island effects disproportionately influence lightning enhancement, potentially by altering storm activity. These patterns improve our understanding of how cities change local climate and highlight potential avenues for mitigation.

The results of this study support the prediction that urban heat island effects influence lightning enhancement; however, we found no evidence that pollution increases lightning strike frequency in urban areas. Our approach could underestimate the cumulative effects of pollution by ignoring lightning enhancement in nearby natural areas. Nonetheless, when considering lightning enhancement over cities themselves, our global analysis effectively separates the contributions of many varied factors, revealing that urban heat island effects are stronger and more consistent than the effects of pollution. Urban heat island effects can disrupt atmospheric stability, leading to thunderstorms due to the increased convection of air masses [3]. Because urban heat island effects are dependent on urban design, efforts to reduce urban heat islands through shifts in urban planning (e.g. green roofs, building orientation or construction materials [43,47,48]) may also reduce lightning enhancement. Unravelling the mechanisms underlying urban heat island effects on lightning enhancement requires a detailed exploration of the physical processes of lightning initiation.

Both regional lightning strike frequency and the differences in precipitation between urban and surrounding natural areas shape lightning enhancement patterns. The effect of regional lightning strike frequency on lightning enhancement suggests that urbanization primarily amplifies lightning frequency where it already occurs rather than creating lightning where it is uncommon. Additionally, the higher rates of lightning enhancement among cities that also exhibited higher precipitation ratios (presumably caused by anthropogenic factors such as urban aerosols [43]) indicate that urbanization could increase lightning strike frequency, in part, by producing more or stronger storms [23,49–54]. Our metric of increased precipitation ratios does not directly measure convection, but it probably captures differences in convective rainfall and overall storm activity. We need further investigation into urbanization, lightning and storm formation to understand the processes underlying these relationships.

Aspects of geography, topography and urbanization also influenced lightning enhancement. These effects suggest that large, lowland cities in tropical regions are the most susceptible to strong lightning enhancement effects. Predictions of future urbanization suggest an increased number of large cities in tropical areas [55], many of which will be at low elevations. Thus, these cities will be particularly likely to produce strong lightning enhancement effects. Cities at low elevations typically have higher temperatures than high-elevation cities, which may exacerbate urban heat island effects on lightning enhancement. Counter to our expectations, coastal cities exhibit less lightning enhancement than inland cities. One possible explanation is that coastal cities exhibit less temperature variation than inland cities due to the thermal buffering of the ocean [56], and fast temperature changes (which were not captured in this study) could produce both more thunderstorms and stronger urban heat island effects [8]. However, this effect was particularly weak and was not apparent in the bivariate analyses or the enhancement strength. Urban planning to reduce urban heat island effects, which has many other benefits, could also reduce the likelihood of lightning enhancement among these growing cities.

The results of this study suggest at least three avenues for further research that would improve our understanding of anthropogenic effects on lightning frequency and distribution. First, large-scale studies of local-scale atmospheric phenomena across more cities could validate the global-scale trends of lightning enhancement in our study (table 1). Second, the effects of urbanization on lightning characteristics (e.g. the fraction of flashes that are ground strikes and the intensity of individual discharges) remain unknown. Finally, examining lightning enhancement among smaller-scale geographic features (e.g. the relevance of urban greenspace) and beyond the boundaries of urban limits (e.g. downwind effects of urbanization) could inform urban planning decisions. Ultimately, continued monitoring will be crucial to understanding how humans shape regional atmospheric phenomena and how those effects will respond to global change.

Ethics. This work did not require ethical approval from a human subject or animal welfare committee.

Data accessibility. Data and code is publicly available through the Cary Institute Figshare at [57]. CHELSA V2 climatic monthly time series were used to assess the temperature and precipitation data (Karger *et al*. [37]) available at [58]. Terra/MODIS Aerosol Optical Depth monthly time series (Kaufman *et al*. [38]) were downloaded from [59]. Aura Nitrogen Dioxide monthly time series (Krotkov & Veefkind [39]). Modern-Era Retrospective analysis for Research and Applications version 2 (MERRA-2) Sulfate Dioxide monthly time series (Gelaro *et al*. [40]). Global Solar Atlas terrain elevation data (Solargis [41]). Global Oceans and Seas shapefile to measure the distance to water bodies (Flanders Marine Institute [42]).The urban area and greenspace were obtained from the Moderate Resolution Imaging Spectroradiometer (MODIS) Land Cover Climate Modeling Grid (CMG) (MCD12C1) Version 6.1 (Friedl & Sulla-Menashe [32]) in [60]. The Annual Population of Urban Agglomerations with 300 000 Inhabitants or More in 2018 by country, 1950–2035, was downloaded from the World Urbanization Prospects 2018 (UN [33]) and found at [61].

Supplementary material is available online [62].

Declaration of AI use. We have not used AI-assisted technologies in creating this article.

Authors' contributions. J.P.N.: data curation, formal analysis, methodology, software, validation, visualization, writing—original draft; S.P.Y.: writing—review and editing; P.M.B.: resources, writing—review and editing; J.C.B.: writing—review and editing; E.M.G.: conceptualization, formal analysis, methodology, supervision, validation, writing—review and editing.

All authors gave final approval for publication and agreed to be held accountable for the work performed therein.

Conflict of interest declaration. We declare we have no competing interests.

Funding. The Smithsonian Tropical Research Institute (STRI) provided logistical support. This work was partially funded by an STRI Earl S. Tupper Fellowship and by grants from the National Science Foundation (DEB-2213246 to S.P.Y.; DEB-2213247 to P.M.B.; and DEB-2213245 to E.M.G.).

References

1. Westcott NE. 1995 Summertime cloud-to-ground lightning activity around major Midwestern urban areas. *J. Appl. Meteorol.* **34**, 1633–1642. (doi:10.1175/1520-0450-34.7.1633)
2. Steiger SM, Orville RE, Huffines G. 2002 Cloud-to-ground lightning characteristics over Houston, Texas: 1989–2000. *J. Geophys. Res.* **107**, ACL(doi:10.1029/2001JD001142)

3. Naccarato KP, Pinto O, Pinto I. 2003 Evidence of thermal and aerosol effects on the cloud-to-ground lightning density and polarity over large urban areas of Southeastern Brazil. *Geophys. Res. Lett*. **30**, 13. (doi:10.1029/2003GL017496)
4. Pinto Jr O, Pinto IRCDA, Neto OP. 2013 Lightning enhancement in the Amazon region due to urban activity. *Am. J. Clim. Change* **2**, 270–274. (doi:10.4236/ajcc.2013.24026)
5. Wang Y, Wan Q, Meng W, Liao F, Tan H, Zhang R. 2011 Long-term impacts of aerosols on precipitation and lightning over the Pearl River Delta megacity area in China. *Atmos. Chem. Phys*. **11**, 12 421–12 436. (doi:10.5194/acp-11-12421-2011)
6. Wang Y, Lu G, Shi T, Ma M, Zhu B, Liu D, Peng C, Wang Y. 2021 Enhancement of cloud-to-ground lightning activity caused by the urban effect: a case study in the beijing metropolitan area. *Remote Sens.* **13**, 1228. (doi:10.3390/rs13071228)
7. Wang H, Shi Z, Wang X, Tan Y, Wang H, Li L, Lin X. 2021 Cloud-to-ground lightning response to aerosol over air-polluted urban areas in china. *Remote Sens.* **13**, 2600. (doi:10.3390/rs13132600)
8. Lal DM, Pawar SD. 2011 Effect of urbanization on lightning over four metropolitan cities of India. *Atmos. Environ.* **45**, 191–196. (doi:10.1016/j.atmosenv.2010.09.027)
9. Lynn BH, Yair Y, Shpund J, Levi Y, Qie X, Khain A. 2020 Using factor separation to elucidate the respective contributions of desert dust and urban pollution to the 4 January 2020 Tel Aviv lightning and flash flood disaster. *J. Geophys. Res*. **125**, 24. (doi:10.1029/2020JD033520)
10. Kar SK, Liou YA, Ha KJ. 2007 Characteristics of cloud-to-ground lightning activity over Seoul, South Korea in relation to an urban effect. *Ann. Geophys*. **25**, 2113–2118. (doi:10.5194/angeo-25-2113-2007)
11. Kar SK, Liou YA, Ha KJ. 2009 Aerosol effects on the enhancement of cloud-to-ground lightning over major urban areas of South Korea. *Atmos. Res*. **92**, 80–87. (doi:10.1016/j.atmosres.2008.09.004)
12. Kar SK, Liou YA. 2014 Enhancement of cloud-to-ground lightning activity over Taipei, Taiwan in relation to urbanization. *Atmos. Res.* **147**, 111–120. (doi:10.1016/j.atmosres.2014.05.017)
13. Soriano LR, de Pablo F. 2002 Effect of small urban areas in central Spain on the enhancement of cloud-to-ground lightning activity. *Atmos. Environ*. **36**, 2809–2816. (doi:10.1016/S1352-2310(02)00204-2)
14. Strikas OM, Elsner JB. 2013 Enhanced cloud-to-ground lightning frequency in the vicinity of coal plants and highways in Northern Georgia, USA. *Atmos. Sci. Lett*. **14**, 243–248. (doi:10.1002/asl2.446)
15. Burke JD, Shepherd M. 2023 The urban lightning effect revealed with geostationary lightning mapper observations. *Geophys. Res. Lett*. **50**, e2022GL102272. (doi:10.1029/2022GL102272)
16. Orville RE, Huffines G, Nielsen-Gammon J, Zhang R, Ely B, Steiger S, Phillips S, Allen S, Read W. 2001 Enhancement of cloud-to-ground lightning over Houston, Texas. *Geophys. Res. Lett*. **28**, 2597–2600. (doi:10.1029/2001GL012990)
17. Orville RE, Huffines GR. 1999 Lightning ground flash measurements over the contiguous United States: 1995–97. *Month. Weather Rev.* **127**, 2693–2703. (doi:10.1175/1520-0493(1999)127<2693:LGFMOT>2.0.CO;2)
18. Twomey SA, Piepgrass M, Wolfe TL. 1984 An assessment of the impact of pollution on global cloud albedo. *Tellus B* **36B**, 356–366. (doi:10.1111/j.1600-0889.1984.tb00254.x)
19. Yau MK, Rogers RR. 1996 *A short course in cloud physics*. Oxford, UK: Elsevier.
20. Stolz DC. 2016 *The simultaneous influence of thermodynamics and aerosols on deep convection and lightning*. Fort Collins, CO: Colorado State University. See http://hdl.handle.net/10217/173332.
21. Thornton JA, Virts KS, Holzworth RH, Mitchell TP. 2017 Lightning enhancement over major oceanic shipping lanes. *Geophys. Res. Lett*. **44**, 9102–9111. (doi:10.1002/2017GL074982)
22. Oke TR. 1982 The energetic basis of the urban heat island. *Quart. J. Royal Meteoro. Soc*. **108**, 1–24. (doi:10.1002/qj.49710845502)
23. Bornstein R, Lin Q. 2000 Urban heat islands and summertime convective thunderstorms in Atlanta: three case studies. *Atmos. Environ.* **34**, 507–516. (doi:10.1016/S1352-2310(99)00374-X)
24. Christian HJ *et al*. 2003 Global frequency and distribution of lightning as observed from space by the optical transient detector. *J. Geophys. Res.* **108**, ACL 4-1–4-15. (doi:10.1029/2002JD002347)
25. Song Y, Semazzi FHM, Xie L, Ogallo LJ. 2004 A coupled regional climate model for the Lake Victoria basin of East Africa. *Int. J. Climatol*. **24**, 57–75. (doi:10.1002/joc.983)
26. Freitas ED, Rozoff CM, Cotton WR, Dias PLS. 2007 Interactions of an urban heat island and sea-breeze circulations during winter over the metropolitan area of São Paulo, Brazil. *Boundary Layer Meteorol*. **122**, 43–65. (doi:10.1007/s10546-006-9091-3)
27. Holle RL, Murphy MJ. 2017 Lightning over three large tropical lakes and the strait of Malacca: exploratory analyses. *Mon. Wea. Rev*. **145**, 4559–4573. (doi:10.1175/MWR-D-17-0010.1)
28. Mushtaq F, Nee Lala MG, Anand A. 2018 Spatio-temporal variability of lightning activity over J&K region and its relationship with topography, vegetation cover, and absorbing aerosol index (AAI). *J. Atmos. Sol. Terr. Phys*. **179**, 281–292. (doi:10.1016/j.jastp.2018.08.011)
29. Kar SK, Liou YA. 2019 Influence of land use and land cover change on the formation of local lightning. *Remote Sens.* **11**, 407. (doi:10.3390/rs11040407)
30. Liu C, Heckman S. 2012 Total lightning data and real-time severe storm prediction. In *Tech. Conf. on Meteorological and Environmental Instruments and Methods of Observation*, Brussels, Belgium, 16–18 October 2012, pp. 1–12.
31. Cummins KL, Murphy MJ, Bardo EA, Hiscox WL, Pyle RB, Pifer AE. 1998 A combined TOA/MDF technology upgrade of the U.S. National Lightning Detection Network. *J. Geophys. Res*. **103**, 9035–9044. (doi:10.1029/98JD00153)
32. Friedl M, Sulla-Menashe D. 2019 *MCD12Q1 MODIS/terra+ aqua land cover type yearly L3 global 500m SIN grid V006*. NASA EOSDIS Land Processes DAAC. (doi:10.5067/MODIS/MCD12Q1.006)
33. United Nations DE, D SAP. 2018 World urbanization prospects: the 2018 revision. New York, NY: United Nations. See https://population.un.org/wup/Download/.
34. He JF, Liu JY, Zhuang DF, Zhang W, Liu ML. 2007 Assessing the effect of land use/land cover change on the change of urban heat island intensity. *Theor. Appl. Climatol*. **90**, 217–226. (doi:10.1007/s00704-006-0273-1)
35. Mendez-Espinosa JF, Belalcazar LC, Morales Betancourt R. 2019 Regional air quality impact of northern South America biomass burning emissions. *Atmos. Environ.* **203**, 131–140. (doi:10.1016/j.atmosenv.2019.01.042)
36. Cohen J. 1992 Quantitative methods in psychology: a power primer. *Psychol. Bull.* **112**, 155–159. (doi:10.1037//0033-2909.112.1.155)
37. Karger DN, Conrad O, Böhner J, Kawohl T, Kreft H, Soria-Auza RW, Zimmermann NE, Linder HP, Kessler M. 2017 Climatologies at high resolution for the earth's land surface areas. *Sci. Data* **4**, 170122. (doi:10.1038/sdata.2017.122)
38. Kaufman YJ, Tanré D, Boucher O. 2002 A satellite view of aerosols in the climate system. *Nature* **419**, 215–223. (doi:10.1038/nature01091)
39. Krotkov NA, Veefkind P. 2016 *OMI/aura nitrogen dioxide (NO_2) total and tropospheric column 1-orbit L2 swath 13x24 km V003*. Greenbelt, MD: Goddard Earth Sciences Data and Information Services Center (GES DISC).

40. Gelaro R *et al*. 2017 The modern-era retrospective analysis for research and applications, version 2 (MERRA-2). *J. Clim*. **30**, 5419–5454. (doi:10.1175/JCLI-D-16-0758.1)
41. Solargis S. 2019 Global Solar Atlas 2.0. A free web-based application developed and operated by the company Solargis s.r.o. on behalf of the World Bank Group, utilizing Solargis data, with funding provided by the Energy Sector Management Assistance Program (ESMAP). See https://globalsolaratlas.info.
42. Flanders Marine Institute. 2021 Maritime boundaries geodatabase: maritime boundaries and exclusive economic zones (200NM), version 11. See https://www.marineregions.org.
43. Shepherd JM, Stallins JA, Jin ML, Mote TL. 2015 Urbanization: impacts on clouds, precipitation, and lightning. *Urban Ecosyst. Ecol.* 1–28. (doi:10.2134/agronmonogr55.c1)
44. Bates D, Maechler M, Bolker B, Walker S, Christensen RHB, Singmann H, Bolker MB. 2015 Fitting linear mixed-effects models using lme4. *J. Stat. Software* **67**, 1–48. (doi:10.18637/jss.v067.i01)
45. Barton K. 2010 MuMIn: multi-model inference. R package version 0.13 (doi:10.32614/CRAN.package.MuMIn)
46. R Core Team. 2013 R: A language and environment for statistical computing. vienna, austria: R foundation for statistical computing. See https://www.R-project.org/.
47. Shahmohamadi P, Che-Ani AI, Ramly A, Maulud KNA, Mohd-Nor MFI. 2010 Reducing urban heat island effects: a systematic review to achieve energy consumption balance. *Int. J. Phys. Sci.* **5**, 626–636. (doi:10.2495/SDP-V5-N4-351-366)
48. Changnon SA. 1992 Inadvertent weather modification in urban areas: lessons for global climate change. *Bull. Am. Meteorol. Soc*. **73**, 619–627. (doi:10.1175/1520-0477(1992)073<0619:IWMIUA>2.0.CO;2)
49. Baik JJ, Kim YH, Chun HY. 2001 Dry and moist convection forced by an urban heat Island. *J. Appl. Meteor*. **40**, 1462–1475. (doi:10.1175/1520-0450(2001)040<1462:DAMCFB>2.0.CO;2)
50. Rozoff CM, Cotton WR, Adegoke JO. 2003 Simulation of St. Louis, Missouri, land use impacts on thunderstorms. *J. Appl. Meteor*. **42**, 716–738. (doi:10.1175/1520-0450(2003)042<0716:SOSLML>2.0.CO;2)
51. Wang C. 2005 A modeling study of the response of tropical deep convection to the increase of cloud condensation nuclei concentration: 1. dynamics and microphysics. *J. Geophys. Res*. **110**, D21. (doi:10.1029/2004JD005720)
52. Martins JA, Silva Dias MAF da, Gonçalves FLT. 2009 Impact of biomass burning aerosols on precipitation in the Amazon: a modeling case study. *J. Geophys. Res*. **114**, D2. (doi:10.1029/2007JD009587)
53. Thielen J, Wobrock W, Gadian A, Mestayer PG, Creutin JD. 2000 The possible influence of urban surfaces on rainfall development: a sensitivity study in 2D in the meso-γ-scale. *Atmos. Res*. **54**, 15–39. (doi:10.1016/S0169-8095(00)00041-7)
54. van den Heever SC, Carrió GG, Cotton WR, DeMott PJ, Prenni AJ. 2006 Impacts of nucleating aerosol on Florida storms. Part I: mesoscale simulations. *J. Atmos. Sci.* **63**, 1752–1775. (doi:10.1175/JAS3713.1)
55. Gupta A. 2002 Geoindicators for tropical urbanization. *Env. Geol*. **42**, 736–742. (doi:10.1007/s00254-002-0551-x)
56. Pamarthi A. 2019 The recent trend of the temperature in major cities of India: a difference between inland areas and coastal areas in the climate change scenario. *Atmos. Sci.* **1**, 1. (doi:10.1017/CBO9780511546013)
57. Narvaez P, Gora E, Yanoviak SP, Bitzer P, Burchfield J. 2024 Code associated with: Effects of urbanization on cloud-to-ground lightning strike frequency: a global perspective. Cary Institute. (doi:10.25390/caryinstitute.26597314)
58. ENVICLOUD. 2024 See https://envicloud.wsl.ch/#/?prefix=chelsa%2Fchelsa_V2%2FGLOBAL%2F.
59. NASA Earth Observations. 2024 Aerosol Optical Thickness. See https://neo.gsfc.nasa.gov/view.php?datasetId=MODAL2_M_AER_OD.
60. Sulla-Menashe D, Friedl M. MODIS/terra+aqua land cover type yearly L3 global 0.05deg CMG V061. NASA EOSDIS land processes distributed active archive center. (doi:10.5067/MODIS/MCD12C1.061). See https:// lpdaac.usgs.gov/products/mcd12c1v061/.
61. United Nations. 2018 World urbanization prospects. See https://population.un.org/wup.
62. Narvaez JP, Bitzer PM, Burchfield JC, Yanoviak SP, Gora EM. 2024 Data from: Effects of urbanization on cloud-to-ground lightning strike frequency: a global perspective. Figshare. (doi:10.6084/m9.figshare.c.7422806)